Efficient acetate sensor in biological media based on a selective Excited State Proton Transfer (ESPT) reaction

Virginia Puente−Muñoz,[a] Jose M. Paredes,[a]* Sandra Resa,[b] Ana M. Ortuño,[b] Eva M. Talavera[a] , Delia Miguel,[a] Juan M. Cuerva[b] and Luis Crovetto[a]*

a. Department of Physical Chemistry, Faculty of Pharmacy, University of Granada, Cartuja Campus, 18071 Granada, Spain. E-mail: luiscrovetto@ugr.es, jmparedes@ugr.es

b. Department of Organic Chemistry, Faculty of Sciences, University of Granada, C. U. Fuentenueva s/n, 18071 Granada, Spain.

Abstract

We have synthesized a new fluoride−containing xanthenic dye able to dynamically and quantitatively detect acetate anion, a biologically relevant analyte, in water. We studied deeply the photophysical properties of the compound and verified its use as an acetate probe in synthetic serum.

Highlights

"On/off" fluorescent dye to detect acetate.

High sensitivity Acetate detection in biological serum is reported.

Acetate ions are important in physiological processes because it participates directly and/or indirectly in cancer metabolism

Keywords

Acetate sensor, Excited State Proton Transfer (ESPT) reaction, fluorescent probe.

1. Introduction

Acetate, the ionized form of acetic acid, is a critical metabolite in fatty acids and carbohydrate metabolism [1]. The importance of acetate in the metabolism goes further than a physiological process as it is directly and/or indirectly involved in cancer metabolism [2, 3], and consequently several acetate role studies about different cancer types can be found in literature [4, 5]. In particular, it is relevant in the colorectal tumor,

one of the most prevalent cancers in the world nowadays. One of the roles acetate has in cancer is that it participates in cancer cells apoptosis [6] and its detection and study could help to achieve a better understanding of cell death mechanism and could also help to discover new tools for colorectal cancer prevention [1, 7].

Due to its biological and physiopathological importance, the availability of new probes to detect acetate *in situ* in biological samples is essential for metabolism research in which acetate is involved. A very successful approach in this field has been the interaction between the probe and the acetate anion by complementary hydrogen bonding [8]. Nevertheless, such kind of interactions can also occur with other anions such as phosphate, iodine, bromide or fluoride [9]. Moreover the nature of this interaction precludes, in general, the use of pure water as solvent owing to the undesirable competition of water with the hydrogen-bond based interaction [10, 11]. To the best of our knowledge there are only two strategies in literature in which water is exclusively used as solvent. First implies chemical derivatization of acetate in basic media followed by gas chromatography analysis [12]. The second one is the use of commercially available kits. These can be based on kinetic processes or the use of enzymes. Nevertheless, they present some drawbacks related with the necessity of clear samples, interferences with either compounds (i.e. –SH containing reagents) or other enzymes present in the samples. Moreover, in all the cases the total acetate anion is determined by derivatization of the compound, which prevents from measuring changes in acetate concentration during the analysis in dynamic samples. In this sense it would be interesting to base the analysis in a parameter which is not affected by turbidity and/or the sample composition and that allows a dynamic detection in real time. Therefore, the challenge in this field is to retain the acetate sensitivity and selectivity in water in a dynamic way. To this end a very different approach is required.

A common feature of all the anions is the acid-base characteristics in water, which in principle can be used to discriminate between them. Within this context, it is known that Excited State Proton Transfer (ESPT) reactions [13] promote changes in fluorescent molecules, which can be detected and related with the presence of the corresponding proton donor/acceptor. ESPT reaction is faster than fluorescence emission and depends on the proton donor/acceptor concentration. Therefore, fluorescence decay lifetime (τ)

can be used to monitor the analyte concentration [14]. This fluorescent parameter (τ) presents several advantages over fluorescence intensity such as independence on the dye concentration or easily differentiation of autofluorescence interferences [15]. Moreover, this approach is fully compatible with water and the selectivity of the transfer process is based on the similarities in pK_a between the dye and the analyte (proton donor/acceptor), which precludes any interference of anions with different acid-base characteristics [16]. The approach is only limited by the existence of the suitable dye with the required pK_a.

Xanthene-based dyes seem to be ideal for this purpose owing to the remarkable photophysical properties they present and the possibility of a fine-tuning of the pK_a. In particular, Tokyo [13, 14, 17, 18] and Granada Green derivatives [19] had previously shown remarkable "on/off" properties and possibility of ESPT, but they present an unsuitable pK_a value of 6-7. Fluorinated Oregon Green xanthenes [20] present a lower pK_a, achieving the optimal situation in which the buffer and the dye have a similar pK_a. Nevertheless the presence of a carboxylic acid in the structure results in complex acid-base equilibriums and consequently complex analysis. Pennsylvania Green compounds [17] are a smart combination of the Tokyo and Oregon Green dyes resulting in an interesting combination of photophysical and acid-base characteristics. However, the simplest one (**1**, Figure 1) presents an undesirable fluorescence in both neutral and anionic structures, which precludes its use as an "on/off" probe.

In this work, we have synthesized new Pennsylvania-Based dyes **2**-**4**, being one of them (**2**) able to quantitatively detect acetate concentration in water. Compound **2** was studied deeply in order to obtain the rate constants involved in the ESPT reaction promoted by acetate, and to verify its use as an acetate probe in synthetic serum.

2. Material and methods

2.1. Synthesis

All reagents were used as purchased from standard chemical suppliers and used without further purification. Reactions involving organometallic compounds were carried out under Ar atmosphere. TLC was performed on aluminium-backed plates coated with silica gel 60 (230-240 mesh) with F254 indicator. The spots were visualized with UV light (254 nm). All chromatography purifications were performed with silica gel 60 (35-70 μm). NMR spectra were measured at room temperature. ^{1}H NMR spectra were recorded at 300, 400, 500 or 600 MHz. Chemical shifts are reported in ppm using residual solvent peak as reference ($CHCl_3$: δ = 7.26 ppm, CH_2Cl_2: δ = 5.32 ppm, CH_3OH: δ = 3.31 ppm). ^{13}C NMR spectra were recorded at 75, 101, 126 or 151 MHz using broadband proton decoupling and chemical shifts are reported in ppm using residual solvent peaks as reference ($CHCl_3$: δ = 77.16 ppm, CH_2Cl_2: δ = 54.0 ppm, CH_3OH: δ = 49.00 ppm). Carbon multiplicities were assigned by DEPT and HSQC techniques. High resolution mass spectra (HRMS) were recorded using EI at 70e V on a Micromass AutoSpec (Waters) or by ESI-TOFF mass spectrometry carried out on a Waters Synapt G2 mass spectrometer.

2.2. Sample preparation

A stock solution of dyes (9×10^{-5} M) in 10^{-3} M NaOH was prepared using Milli-Q water. For samples preparation in acetate buffer solutions, sodium acetate and acetic acid (both Sigma puriss. p.a.) were used in appropriate amounts to obtain the required pH and dye concentration. Solutions without buffer were prepared using NaOH and $HClO_4$ (0.01 M) both from Sigma-Aldrich, spectroscopic grade. All the solutions were prepared using Milli-Q water as a solvent. All of the chemicals were used as received without further purification. The solutions were kept cool in the dark when not in use to avoid possible deterioration through exposure to light and heat.

2.3. Photophysics Studies

Absorption spectra were recorded using a Perkin-Elmer Lambda 650 UV/Vis spectrophotometer with a Peltier temperature controller. Steady-state fluorescence emission spectra were collected using a JASCO FP-8300 spectrofluorometer equipped with a 450−W xenon lamp for excitation with an ETC-273T temperature controller. All measurements were recorded at room temperature using 10 × 10 mm cuvettes. The pH of the solutions was measured immediately before and after recording each spectrum.

Fluorescence decay traces of solutions were recorded by the single-photon timing method using a FluoTime 200 fluorometer (PicoQuant, Inc.) [15, 21]. The excitation was achieved using a LDH−485 and LDH−440 (PicoQuant, Inc.), and the observation was performed through a monochromator at 510, 515, 520 and 525 nm. The pulse repetition rate was 20 MHz. Fluorescence decay histograms were collected in 1320 channels using 10 × 10 mm cuvettes. The time increment per channel was 37 ps. Histograms of the instrument response functions (using a LUDOX scatterer) and sample decays were recorded until they typically reached 2×10^4 counts in the peak channel. Three fluorescence decays were recorded for all of the samples. The fluorescence decay traces were individually analyzed using an iterative deconvolution method with exponential models using FluoFit software (PicoQuant).

2.4. FLIM analysis

FLIM images were collected by a Pico Quant MicroTime 200 microscope system with an excitation source of LDH-485 laser. The light beam passed through a dichroic mirror (510dcxr, Chroma) and through the oil immersion objective (1.4 NA, 100×) specific to an inverted microscope system (IX-71, Olympus). After passing the immersion objective, the fluorescence light was filtered by a long-pass filter (500LP, AHF/Chroma) and directed to a 75-µm confocal aperture. The light was transmitted to a FF01-520/35 bandpass filter (Thorlabs) and focused on single-photon avalanche diodes (SPCM-AQR 14, Perkin Elmer). The data were collected by a TimeHarp 200 TCSPC module (PicoQuant) and raw Fluorescence lifetime images were acquired by a scanner with 512 x 512 pixels resolution. To obtain the fitted FLIM images, it was realized a binning of 2 x 2 in SymphoTime software and the matrix data were exported and analyzed by a home-coded *Fiji* ([*Fiji Is Just*] *ImageJ*) program [22]. For this aim, and firstly of all, outliers data

points were removed using a selective median filter that replaces a pixel by the median of the pixels in the surrounding (s.d. = 7 pixels) if it deviates from the median by more than a certain value. Finally, in order to achieve a larger number of counts in each pixel, it was done a binning of 4 x 4 and later, a Gaussian smoothing function (s.d. = 1 pixel) filters were applied.

3. Results and Discussions

The careful selection of the pK_a of the fluorescent probe is crucial for the acetate anion sensing. For this reason we decided to use 2,7-difluorinated xanthene as fluorescent core owing to the inductive effect of fluorine atoms and the consequent increase in the acidity of xanthenes derivatives. We have recently reported that the pK_a of a functionalized xanthene can be also fine tuned with a judicious selection of the substitution at C-9 [19]. It is also known that the "on/off" characteristics can be modulated by the substituents in the C-9 position [18]. After some synthetic effort we found that Pennsylvania-type xanthene **2** presented the best photophysical and acid-base characteristics for our objective. Based on our previously described methodology [16] we synthesized compounds **1**-**4** in good yields as it is reported in the Electronic Supporting Information (ESI) [18, 23].

1: R^1 = Me, R^2 = H
2: R^1 = Me, R^2 = OMe
3: R^1 = OMe, R^2 = Me
4: R^1 = OMe, R^2 = *t*Bu

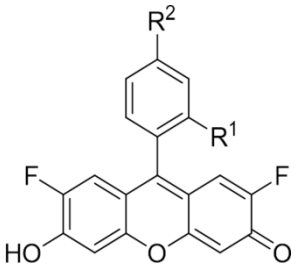

Scheme 1: Molecular structure of the synthesized compounds

Absorption measurements for compound **2** in water strongly depend on the pH (Figure 1). Spectra showed a maximum at 492 nm at higher pH values measured (corresponding to the anion form) and two maxima (450/478 nm) at lower pH values (corresponding to the neutral form).The isosbestic point suggests a chemical equilibrium between two species; i.e. the neutral and anion forms as chemical structures suggest. From those spectra the pK_a and the molar absorption coefficients ε_I (λ_{abs}) could be extracted using non-lineal global fitting of absorbance surface *vs* pH and λ_{abs} [24] (see SI). Experimental

pK_a corresponds to 4.04 ± 0.02, around three units lower than the non-fluoride compounds [19, 25] and reasonably close to the acetate pK_a value (4.76).

Figures 1B and 1C show plots of individual absorbance at different pH values and the recovered values of molar absorption coefficients of both neutral (ε_N) and anionic form (ε_A) in the absence of acetate buffer.

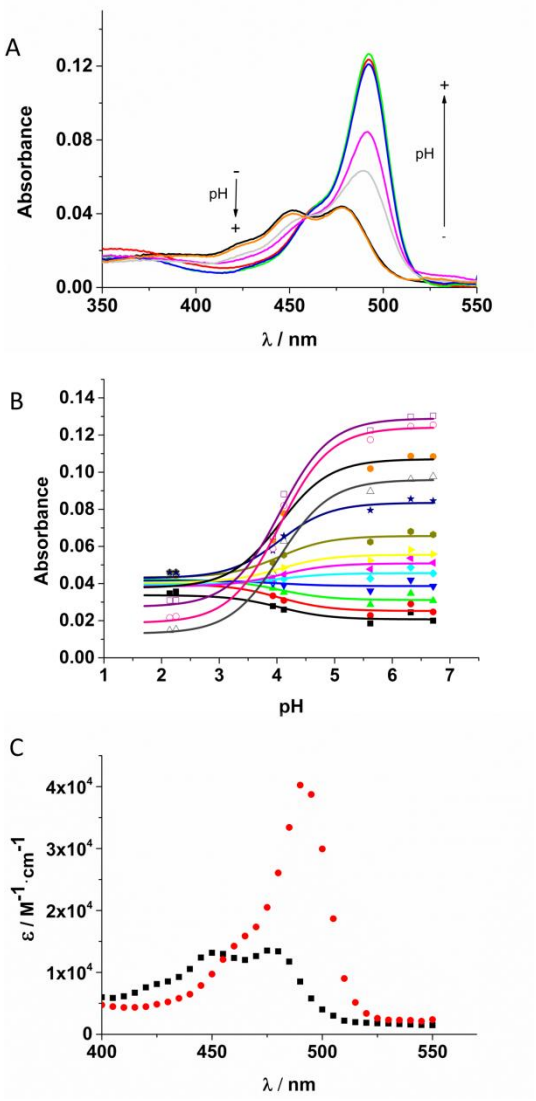

Figure 1: A) Absorption spectra of compound **2** (3.2×10^{-6} M) at different pH values (from 2.14 to 6.71). B) Curves generated by fitting the individual A (λ_{abs}) versus pH data. C) Recovered molar absorption coefficients versus wavelength for the neutral (black) and anionic (red) form of compound **2**

As can be observed, the shape of the absorption coefficients is similar to the previous dyes as shown in bibliography [17-19]. For the anion, it is shown a maximum at 492 nm

and a shoulder at around 460 nm. The neutral absorption coefficient shows two maxima at 450 and 480 nm. However, it is almost three times lower than the anion maximum.

A steady-state fluorescence study resulted in the emission spectra profiles corresponding to the two prototropic species involved in the chemical equilibrium. The anionic species have an emission maximum at 515 nm and the neutral emission maxima are centered at 510 nm (see Figure S4 in SI). Moreover, the quantum yields (Φ) of every species were calculated: 0.65 for the anionic one and a very low value of 0.02 for the neutral one, which is an ideal photophysical characteristic for our purpose.

We recovered the pk_a in the excited state (pK_a^*) by steady-state fluorescence using high acetate concentration so that buffer mediated ESPT reaction would occur during the excited lifetime. The resulting pK_a^* (4.42 ± 0.07) was similar to the pK_a in the ground state (Figure S5). Figure 2 shows the emission spectra of compound **2** at different pH values. It is remarkable the very low intensity values at lower pH with a decrease of about 160 times in the fluorescence signal, evidencing the "on/off" character of the dye.

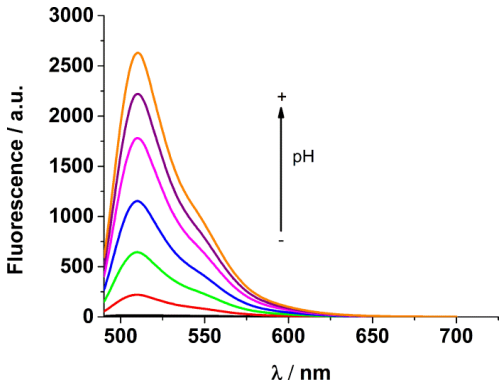

Figure 2: Fluorescence emission spectra of compound **2** (6×10^{-6} M) in acetate (400 mM) solution at different pH values (from 1.37 to 7.79)

Finally, using time-resolved fluorescence, we recovered the decay times. In concordance with steady-state emission, anion species decay time (3.30 ns) is higher than neutral one, becoming almost insignificant (0.02 ns).

Some xanthene derivatives can undergo an ESPT reaction when an appropriate proton donor/acceptor, as acetate, is present. These reactions can modify the steady-state or

time-resolved fluorescence signal. Important experimental information of the ESPT reaction mechanism is accessible through time-resolved fluorescence measurements, by which the kinetic behavior of the system in the excited state can be obtained. Figure 3A shows the scheme involved in the ESPT reaction and fluorescence emission for the two species of compound **2** present at the pH range studied, considering a causal, linear, time-invariant, intermolecular system. The theory of buffer-mediated ESPT reactions has been well established (See SI) [26].

Firstly, we measured compound **2** in absence of acetate buffer. We realized a global analysis of 40 curves corresponding to C^B = 0 mM, at pH range from 4.28 to 6.65, at λ_{ex} = 485 and 440nm and λ_{em} = 510, 520, 530, 540 and 550 nm, providing pH independent reliable decay time estimations: τ_1 = 0.021 ± 0.003 ns and τ_2 = 3.300 ± 0.002 ns (χ_g^2 = 1.176). This behavior confirms that in the absence of acetate ions the buffer-mediated ESPT reaction does not occur. When the pH was much higher than the pK_a value, only the anion species is present. In this condition, fluorescence decay was given by a monoexponential function with the decay time τ_2 = 3.300 ± 0.002 ns. At high pH values the proton concentration is very low, and hence the reprotonation reaction in the excited state is very slow and does not compete with the radiative constant. Therefore, this decay time unequivocally defines a value for $k_{02} = 1/\tau_2$. Decreasing the pH the neutral species were also presented, being the main form at pH values lower than the pK_a. However, the anionic form is preferentially excited at λ_{ex} = 485 nm, due to its large molar absorption coefficient. Moreover the higher quantum yield of anionic species, as well as the low fluorescence quantum yield of the neutral form ("on/off"), makes the fluorescence of this latter one difficult to detect. Although such shorter decay time appears at lower values of pH (pH below 3.8) results in a very small $\alpha_1$contribution in the full decay time. By using λ_{ex} = 440 nm, the neutral form was preferentially excited, and the short decay time (τ_1 = 0.021 ± 0.003 ns) is detectable even at higher pH values (pH higher than 4.50); but keeping in any case a small α_1 contribution. In contrast, the τ_1 decay time may not be specifically assigned to the neutral, k_{01}, radiative constant because this decay time also contains the excited-state dissociation rate constant k_{21}. From the global analyses of decay traces collected in the absence of acetate buffer, we

estimated a value for k_{02} = (3.02 ± 0.01) × 10^8 s^{-1} and for the sum of rate constants (k_{01} + k_{21}) = (5.25 ± 0.71) × 10^{10} s^{-1}.

In order to fully describe the ESPT reaction mediated by acetate buffer the following fluorescence decay surface was collected: pH range from 3.11 to 8.05, and different C^B (0, 21, 85, 170, 200, 340 and 400 mM) as a function of λ_{em} (510, 520, 530, 540 and 550 nm), with λ_{ex} of 485 and 440 nm.

The complete decay surface was analyzed by using the global analysis (GA) approach, which allows the direct determination of the underlying rate constants k_{ij} [26, 27]. Recovered decay times were fit to equation S7-12 in order to obtain the kinetic constants of the proton transfer reaction in the excited state (Figure 3B).

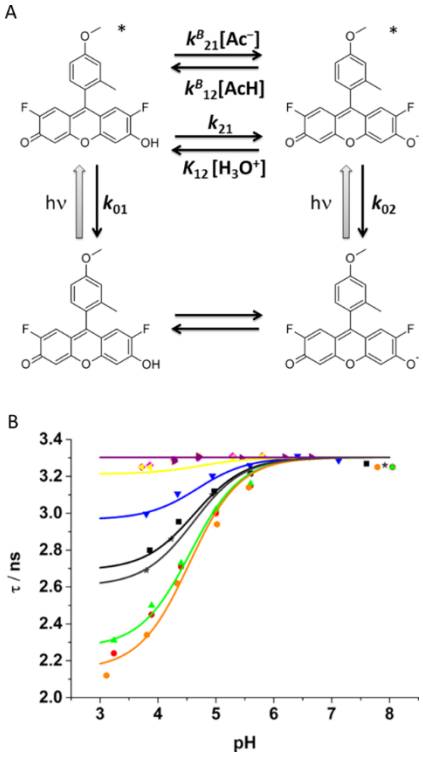

Figure 3: A) Kinetic model of ground- and excited-state proton-transfer reactions of compound **2** in presence of acetate buffer. B) Global fitting (solid lines) of the theoretical equations (eqs S7−S12 in the Supporting Information) to the decay times at different acetate buffer concentrations (0, 21, 85, 170, 200, 340 and 400 mM) and pH values (3.17-8.05)

Rate Constant	**Value**
(k_{01}+k_{21}) / s^{-1}	5.25 (± 0.71) × 10^{10}
k_{02} / s^{-1}	3.02 (± 0.01) × 10^8
k^B_{12} / M^{-1} s^{-1}	4.07 (± 0.12) × 10^8

k_{21}^{B} / M^{-1} s^{-1}	1.99 ($\pm$ 0.34) $\times$ 10^{11}

Table 1: Recovered ESPT rate constant values from the Global Analysis of the Fluorescence decays of Figure 3B.

The good fitting obtained provided estimations, compiled in Table 1, for all the rate constants in Figure 3A. The rate constant values clearly show the much faster deactivation of the neutral form, around two orders of magnitude more rapid than the anion deactivation, which causes the fluorescence being dominated by the anion emission. This correspondence of the simulated curves with the decay times obtained and the sensitivity toward the acetate concentration establishes **2** as an appropriate dye for screening the concentration of acetate at pH around 4.

In order to study the specific response of the dye to acetate in biological samples, we also investigated the potential interference by the presence of other anions presented in serum (pyruvate, glucose, phosphate, bicarbonate and fluoride). No changes in the fluorescence of the dye were found in the presence of these anions except from fluoride, where was observed a slight effect, but without significance in biological samples (see SI).

To take advantage of these results, we checked the capability of the dye to determine acetate in biological samples trough Fluorescence Lifetime Imaging Microscopy (FLIM) using synthetic serum. As monoexponential behavior in decay traces is a useful property for a fluorescence-lifetime based sensor dye, we selected a pH value in which **2** had monoexponential decay in the presence of acetate in order to obtain higher sensitivity. To mimic the liquid biopsies, we used commercial solution of Dulbecco´s modified Eagle´s medium (DMEM) (Sigma-Aldrich D6546) containing inorganic salts, aminoacids, vitamins, high glucose, and other components at different acetate concentration ranging from 15 mM to 120 mM at pH 4.00. To recover the FLIM images, a biexponential function model was used to analyze the decay in each pixel. Shorter decay time was fixed at 1.5 ns that include the background signal of the medium autofluorescence, as well as the possible dye-matrix interactions. The longer decay time was freely fitted being tuned by the acetate concentration. Figure 4A shows the FLIM images representing the dependent decay times recovered at different acetate concentration.

By using an arbitrary color scale the difference in the decay times can be appreciated by change in the colors. Figure 4B shows the respective histograms recovered from Figure 4A.

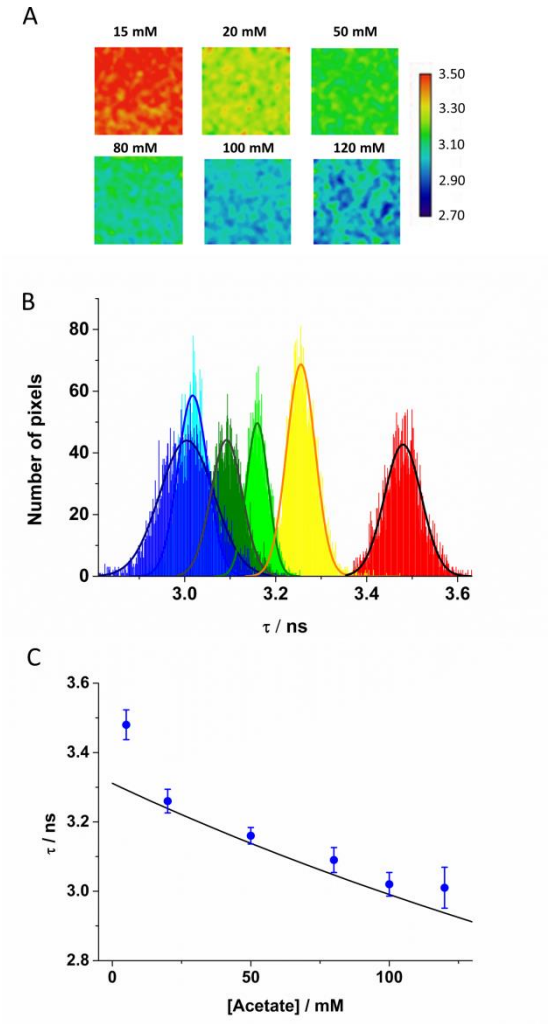

Figure 4: A) FLIM images from compound **2** in DMEM medium with different acetate concentration at pH = 4.00. B) Histograms of lifetimes recovered from Figure 4A. C) Decay time (dot) of the dye in DMEM medium at pH 4.00 obtained from FLIM images and recovered lifetime (line) from the kinetic constants. Scale bars represent the standard deviation.

The average lifetimes of FLIM were also recovered and are shown in Figure 4C, joint with the lifetimes predicted by the kinetic constants at pH 4.00. Even using samples with a complex matrix, the similarity between the lifetime predicted and the experimental is staggering.

4. Conclusions

In summary, a new fluorescent compound **2** has been synthesized, allowing acetate determination in biological samples using fluorescence decay time sensors.

We recovered the kinetic constants of the species involved in the chemical equilibrium presented in the pH range of interest. Finally, to inspect its future application as acetate sensor in liquid biopsies, we checked the ability of this new dye to detect acetate concentration changes using synthetic serum by FLIM. The results were very similar to the decay times predicted by the kinetic constants. Futhermore, it is remarkable that, under the conditions of the experiments performed in this work, the dye achieved the millimolar order sensitivity.

Acknowledgements

Authors gratefully thank to Professor Jose Maria Alvarez-Pez his review and valuable comments.

[†]Dedicated to the memory of Professor Pedro Martinez de las Parras

Funding

This research was funded by MINECO-FEDER funded Grant CTQ2014-53598 and Junta Andalucia FQM2012-790.

Appendix A. Supplementary data

Notes and references

[1] Z.T. Schug, B. Peck, D.T. Jones, Q.F. Zhang, S. Grosskurth, I.S. Alam, et al., Acetyl-CoA Synthetase 2 promotes acetate utilization and maintains cancer cell growth under metabolic stress, Cancer Cell, 27(2015) 57-71.
[2] S.A. Comerford, Z. Huang, X. Du, Y. Wang, L. Cai, A.K. Witkiewicz, et al., Acetate dependence of tumors, Cell, 159(2014) 1591-602.
[3] M. Yoshimoto, A. Waki, Y. Yonekura, N. Sadato, T. Murata, N. Omata, et al., Characterization of acetate metabolism in tumor cells in relation to cell proliferation: Acetate metabolism in tumor cells, Nuclear Medicine and Biology, 28(2001) 117-22.
[4] A.J. Lakhter, J. Hamilton, R.L. Konger, N. Brustovetsky, H.E. Broxmeyer, S.R. Naidu, Glucose-independent acetate metabolism promotes melanoma cell survival and tumor growth, Journal of Biological Chemistry, 291(2016) 21869-79.

[5] T. Mashimo, K. Pichumani, V. Vemireddy, K.J. Hatanpaa, D.K. Singh, S. Sirasanagandla, et al., Acetate is a bioenergetic substrate for human glioblastoma and brain metastases, Cell, 159(2014) 1603-14.
[6] C. Marques, C.S.F. Oliveira, S. Alves, S.R. Chaves, O.P. Coutinho, M. Corte-Real, et al., Acetate-induced apoptosis in colorectal carcinoma cells involves lysosomal membrane permeabilization and cathepsin D release, Cell Death & Disease, 4(2013).
[7] C.A. Lyssiotis, L.C. Cantley, Acetate fuels the cancer engine, Cell, 159(2014) 1492-4.
[8] C. Suksai, T. Tuntulani, Chromogenic anion sensors, Chemical Society Reviews, 32(2003) 192-202.
[9] A.K. Mahapatra, G. Hazra, J. Roy, P. Sahoo, A simple coumarin-based colorimetric and ratiometric chemosensor for acetate and a selective fluorescence turn-on probe for iodide, Journal of Luminescence, 131(2011) 1255-9.
[10] W.W. Huang, H. Lin, H.K. Lin, Fluorescent acetate-sensing in aqueous solution, Sensors and Actuators B-Chemical, 153(2011) 404-8.
[11] Y. Jiang, L.L. Sun, G.Z. Ren, X. Niu, Z.Q. Hu, A novel colorimetric and fluorescent iminocoumarin-based chemosensor for acetate ion and its application to living cell imaging, Talanta, 146(2016) 732-6.
[12] S. Tumanov, V. Bulusu, E. Gottlieb, J.J. Kamphorst, A rapid method for quantifying free and bound acetate based on alkylation and GC-MS analysis, Cancer & Metabolism, 4(2016).
[13] J.M. Paredes, M.D. Giron, M.J. Ruedas-Rama, A. Orte, L. Crovetto, E.M. Talavera, et al., Real-time phosphate sensing in living cells using Fluorescence Lifetime Imaging Microscopy (FLIM), Journal of Physical Chemistry B, 117(2013) 8143-9.
[14] J.M. Paredes, L. Crovetto, R. Rios, A. Orte, J.M. Alvarez-Pez, E.M. Talavera, Tuned lifetime, at the ensemble and single molecule level, of a xanthenic fluorescent dye by means of a buffer-mediated excited-state proton exchange reaction, Physical Chemistry Chemical Physics, 11(2009) 5400-7.
[15] J.R. Lakowicz, Principles of Fluorescence Spectroscopy, 3rd ed.: Springer; 2006.
[16] S. Resa, A. Orte, D. Miguel, J.M. Paredes, V. Puente-Munoz, R. Salto, et al., New dual fluorescent probe for simultaneous biothiol and phosphate bioimaging, Chemistry-A European Journal, 21(2015) 14772-9.
[17] L.F. Mottram, S. Boonyarattanakalin, R.E. Kovel, B.R. Peterson, The Pennsylvania green fluorophore: A hybrid of Oregon Green and Tokyo Green for the construction of hydrophobic and pH-insensitive molecular probes, Organic Letters, 8(2006) 581-4.
[18] Y. Urano, M. Kamiya, K. Kanda, T. Ueno, K. Hirose, T. Nagano, Evolution of fluorescein as a platform for finely tunable fluorescence probes, Journal of the American Chemical Society, 127(2005) 4888-94.
[19] A. Martinez-Peragon, D. Miguel, A. Orte, A.J. Mota, M.J. Ruedas-Rama, J. Justicia, et al., Rational design of a new fluorescent 'ON/OFF' xanthene dye for phosphate detection in live cells, Organic & biomolecular chemistry, 12(2014) 6432-9.
[20] A. Orte, R. Bermejo, E.M. Talavera, L. Crovetto, J.M. Alvarez-Pez, 2',7'-Difluorofluorescein excited-state proton reactions: Correlation between time-resolved emission and steady-state fluorescence intensity, Journal of Physical Chemistry A, 109(2005) 2840-6.
[21] D. O'Connor, D. Phillips, Time-correlated single photon counting: Academic Press; 1984.
[22] J. Schindelin, I. Arganda-Carreras, E. Frise, V. Kaynig, M. Longair, T. Pietzsch, et al., Fiji: an open-source platform for biological-image analysis, Nature Methods, 9(2012) 676-82.
[23] A. Martinez-Peragon, D. Miguel, R. Jurado, J. Justicia, J.M. Alvarez-Pez, J.M. Cuerva, et al., Synthesis and photophysics of a new family of fluorescent 9-alkyl-substituted xanthenones, Chemistry, 20(2014) 447-55.
[24] J. Yguerabide, E. Talavera, J.M. Alvarez, B. Quintero, Steady-state fluorescence method for evaluating excited-state proton reactions - Application to fluorescein, Photochemistry and Photobiology, 60(1994) 435-41.

[25] L. Crovetto, J.M. Paredes, R. Rios, E.M. Talavera, J.M. Alvarez-Pez, Photophysics of a xanthenic derivative dye useful as an 'on/off' fluorescence probe, Journal of Physical Chemistry A, 111(2007) 13311-20.
[26] L. Crovetto, A. Orte, E.M. Talavera, J.M. Alvarez-Pez, M. Cotlet, J. Thielemans, et al., Global compartmental analysis of the excited-state reaction between fluorescein and (+-)-N-acetyl aspartic acid, Journal of Physical Chemistry B, 108(2004) 6082-92.
[27] N. Boens, N. Basaric, E. Novikov, L. Crovetto, A. Orte, E.M. Talavera, et al., Identifiability of the model of the intermolecular excited-state proton exchange reaction in the presence of pH buffer, Journal of Physical Chemistry A, 108(2004) 8180-9.

SUPPORTING INFORMATION

Efficient acetate sensor in biological media based on a selective Excited State Proton Transfer (ESPT) Reaction

V. Puente-Muñoz,[a] J.M. Paredes,[a] R. Resa,[b] A. M. Ortuño,[b] E. M. Talavera[a] *D. Miguel,[a] J.M. Cuerva,[b] L. Crovetto[a]*

[a]*Department of Physical Chemistry, Faculty of Pharmacy, University of Granada, Cartuja Campus, 18071 Granada, Spain.*

[b]*Department of Organic Chemistry, Faculty of Sciences, University of Granada, C. U. Fuentenueva s/n, 18071 Granada, Spain.*

SYNTHETIC PART

General details

All reagents were used as purchased from standard chemical suppliers and used without further purification. TLC was performed on aluminium-backed plates coated with silica gel 60 (230-240 mesh) with F254 indicator. The spots were visualized with UV light (254 nm). All chromatography purifications were performed with silica gel 60 (35-70 µm). NMR spectra were measured at room temperature. ^{1}H NMR spectra were recorded at 300, 400, 500 or 600 MHz. Chemical shifts are reported in ppm using residual solvent peak as reference ($CHCl_3$: δ = 7.26 ppm, CH_2Cl_2: δ = 5.32 ppm, (CH_3OH: δ = 3.31 ppm). Data are reported as follows: chemical shift, multiplicity (s: singlet, d: doublet, t: triplet, q: quartet, quint: quintuplet, hept: heptuplet, m: multiplet, dd: doublet of doublets, dt: doublet of triplets, td: triplet of doublets, bs: broad singlet), coupling constant (*J* in Hz) and integration; ^{13}C NMR spectra were recorded at 75, 101, 126 or 151 MHz using broadband proton decoupling and chemical shifts are reported in ppm using residual solvent peaks as reference ($CHCl_3$: δ = 77.16 ppm, CH_2Cl_2: δ = 54.0 ppm, (CH_3OH: δ = 49.00 ppm). Carbon multiplicities were assigned by DEPT and HSQC techniques. High resolution mass spectra (HRMS) were recorded using EI at 70eV on a Micromass AutoSpec (Waters) or by ESI-TOFF mass spectrometry carried out on a Waters Synapt G2 mass spectrometer. Known compounds **1[1]**, **6[2]** were isolated as pure samples and showed NMR spectra matching those of the reported ones.

Synthesis

The corresponding synthesis was accomplished employing a very simple methodology [3-4] using as a key step a nucleophilic addition of an organolithium derivative to the corresponding MOM-protected 2,7-difluoroxhanthenone derivative **5** (Scheme 1).

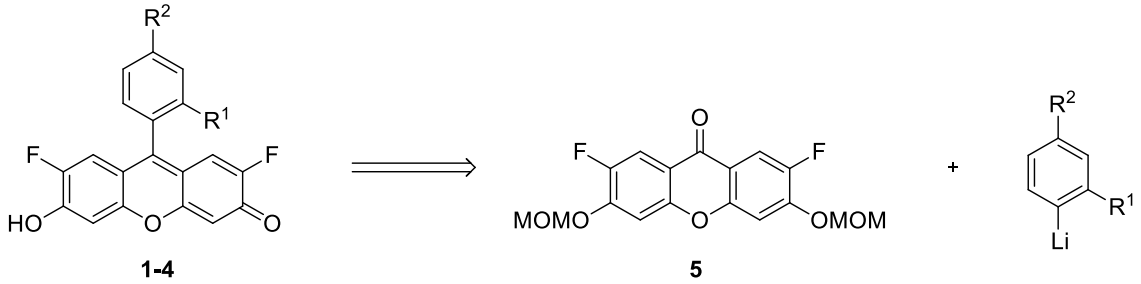

Synthesis of compound 5:

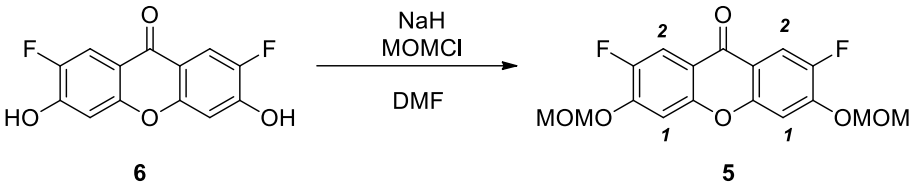

Compound **6[2]** (930 mg, 3.5 mmol) was dissolved in DMF dry (10 mL) and then NaH (703 mg, 17.6 mmol) was added. After stirring for 15 minutes the solution was treated with MOMCl (1.1 mL, 14.0 mmol) and the mixture was stirred at room temperature for 3 h. It was then diluted with EtOAc (20 mL), washed with saturated HCl (aq) (2 x 15 mL), dried over anhydrous Na_2SO_4 and the solvent removed under reduced pressure. The residue was purified by flash chromatography (EtOAc/Hexane mixtures) to give the corresponding protected ketone **5** in a 89 % yield, showing the following spectrocopic data: **^{1}H NMR (500 MHz, $CDCl_3$)** δ 7.94 (d, *J* = 10.6 Hz, 2H, ***H₂***), 7.26 (d, *J* = 6.6 Hz, 2H, ***H₁***), 5.35 (s, 4H, *O-CH₂-O*), 3.55 (s, 6H, *O-CH₃*). **^{13}C NMR (126 MHz, $CDCl_3$)** δ 174.7 (t, *J* = 2.1 Hz, C), 153.5 (d, *J* = 1.4 Hz, C), 151.2 (d, *J* = 13.3 Hz, C), 150.1 (d, *J* = 247.2 Hz, C), 115.5 (d, *J* = 6.2 Hz, C), 112.1 (d, *J* = 20.7 Hz, CH), 104.9 (s, CH), 95.5 (s, CH_2), 56.9 (s, CH_3). **HRMS (ESI):** *m/z* $[M-H]^+$ calcd for $C_{17}H_{15}F_2O_6$: 353.0837; found: 353.0837.

General procedure for the synthesis of compounds 1-4:

A solution of the corresponding bromoaryl derivative (0.2 mmol, 1 eq.) in THF (2 mL) at −78ºC, was treated with *n*-BuLi (0.22 mmol, 1.1 eq). After keeping the reaction at that temperature for 20 minutes ketone **5** (0.1 mmol, 0.5 eq) was added to the solution. Then, the mixture was stirred at −78ºC for 15 minutes and after allowed to reach room temperature. The reaction was monitorized by TLC and after consumption of ketone **5** and then HCl (10%) was added promoting and a colour change from pale yellow to orange. Finally solvent was removed under reduced pressure and residue was submitted to flash chromatography in CH_2Cl_2: MeOH mixtures, affording compounds **1**-**4**, whose spectroscopic data are reported below:

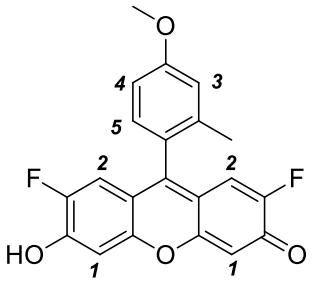

Compound 2: Orange solid obtained in 62 % yield. **^{1}H NMR (500 MHz, MeOD)** δ 7.16 (d, *J* = 8.5 Hz, 1H, H_5), 7.08 (d, *J* = 2.5 Hz, 1H, H_3), 7.03 (dd, *J* = 8.5, 2.5 Hz, 1H, H_4), 6.89 (d, *J* = 7.1 Hz, 2H, H_1), 6.81 (d, *J* = 11.1 Hz, 2H, H_2), 3.92 (s, 3H, -OCH_3), 2.04 (s, 3H, -CH_3). **^{13}C NMR (126 MHz, MeOD)** δ 162.6 (s, C), 156.4 (s, C), 155.6 (s, C), 154.5 (d, *J* = 249.5 Hz, C), 148.1 (s, C), 139.0 (s, C), 131.4 (s, CH), 125.3 (s, C), 117.2 (s, CH), 116.1 (d, *J* = 8.0 Hz, C), 113.1 (s, CH), 113.0 (d, *J* = 22.1 Hz, CH), 106.2 (d, *J* = 4.0 Hz, CH), 55.9 (s, CH_3), 19.9 (s, CH_3). **HRMS (EI, 70 eV):** *m/z* $[M]^+$ calcd for $C_{21}H_{14}F_2O_4$: 368.0860; found: 368.0860.

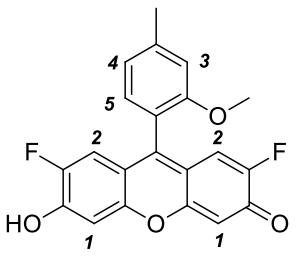

Compound 3: Orange solid obtained in 68 % yield. **^{1}H NMR (500 MHz, MeOD)** δ 7.14 (d, *J* = 8.4 Hz, 1H, *H₅*), 7.06 (d, *J* = 2.5 Hz, 1H, *H₃*), 7.01 (dd, *J* = 8.4, 2.6 Hz, 1H, *H₄*), 6.67 (d, *J* = 7.5 Hz, 2H, *H₁*), 6.66 (d, *J* = 11.5 Hz, 2H, *H₂*), 3.92 (s, 3H, -*OCH₃*), 2.05 (s, 3H, -*CH₃*).**^{13}C NMR (126 MHz, MeOD)** δ 170.94 (d, *J* = 17.0 Hz), 160.81 (s), 156.14 (s), 155.4 (s), 154.96 (d, *J* = 249.5 Hz), 137.33 (s), 129.81 (s), 124.78 (s), 115.58 (s), 111.36 (s), 110.48 (d, *J* = 22.4 Hz), 110.44 (d, *J* = 8.3 Hz), 104.71 (d, *J* = 5.4 Hz), 54.45 (s), 18.43 (s). **HRMS (ESI):** *m/z* $[M\text{-}Na]^+$ calcd for $C_{21}H_{14}F_2NaO_4$: 391.0752; found: 391.0743.

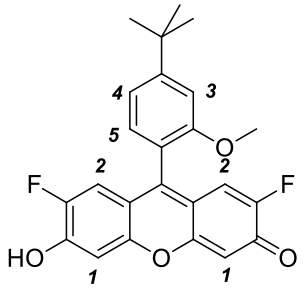

Compound 4: Orange solid obtained in 54 % yield. **^{1}H NMR (600 MHz, MeOD)** δ 7.28 (d, *J* = 1.6 Hz, 1H, *H₃*), 7.27 (dd, *J* = 7.8 Hz, *J* = 1.6 Hz, 1H, *H₄*), 7.15 (d, *J* = 7.8 Hz, 1H, *H₅*), 6.71 (d, *J* = 11.6 Hz, 2H, *H₂*), 6.64 (d, *J* = 7.5 Hz, 2H, *H₁*), 3.77 (s, 3H, -*OCH₃*), 1.46 (s, 9H, *t*Bu). **^{13}C NMR (151 MHz, MeOD)** δ 172.3 (d, *J* = 17.8 Hz, C), 157.8 (s, C), 157.5 (s, C), 156.8 (s, C), 156.2 (d, *J* = 248.9 Hz, C), 155.0 (t, *J* = 5.2 Hz, C), 131.1 (s, CH), 120.3 (s, C), 118.9 (s, CH), 112.2 (d, *J* = 22.5 Hz, CH), 111.9 (d, *J* = 8.6 Hz, C), 110.0 (s, CH), 105.9 (d, *J* = 5.2 Hz, CH), 56.1 (s, CH_3), 36.2 (s, C), 31.7 (s, CH_3). **HRMS (EI, 70 eV):** *m/z* $[M]^+$ calcd for $C_{24}H_{20}F_2O_4$: 410.1330; found: 410.1333.

^{1}H-NMR:

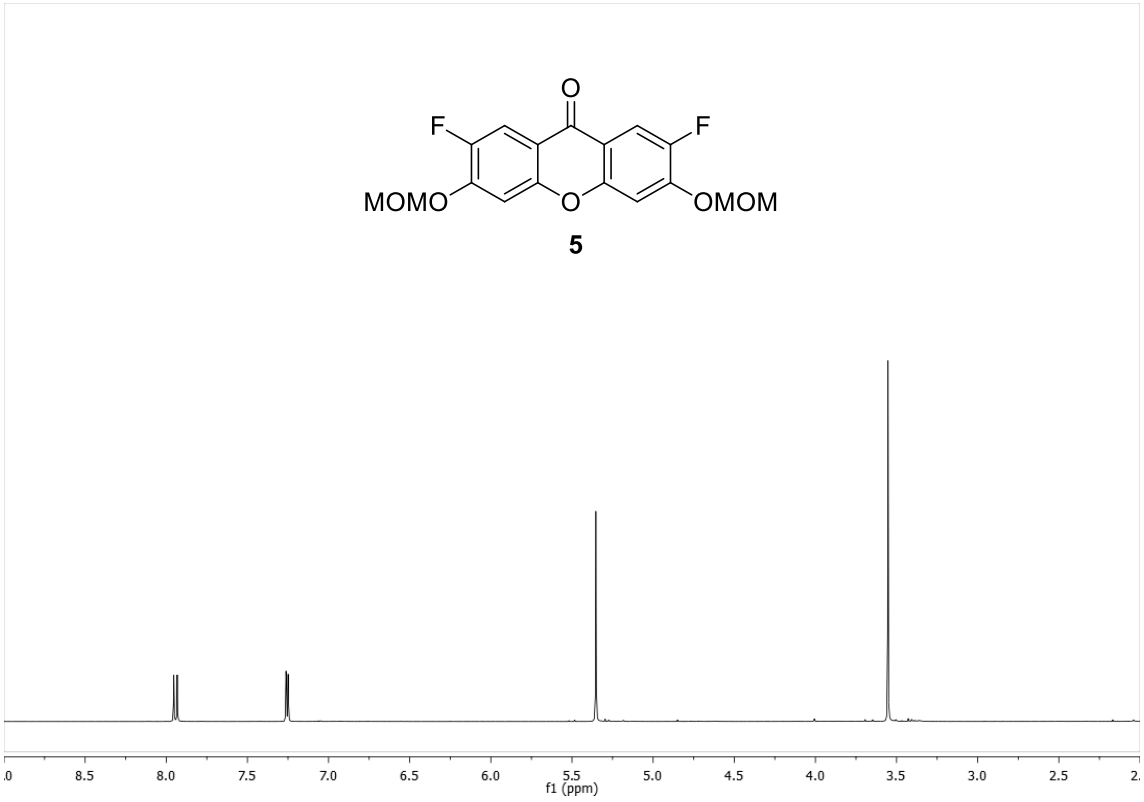

^{13}C-NMR:

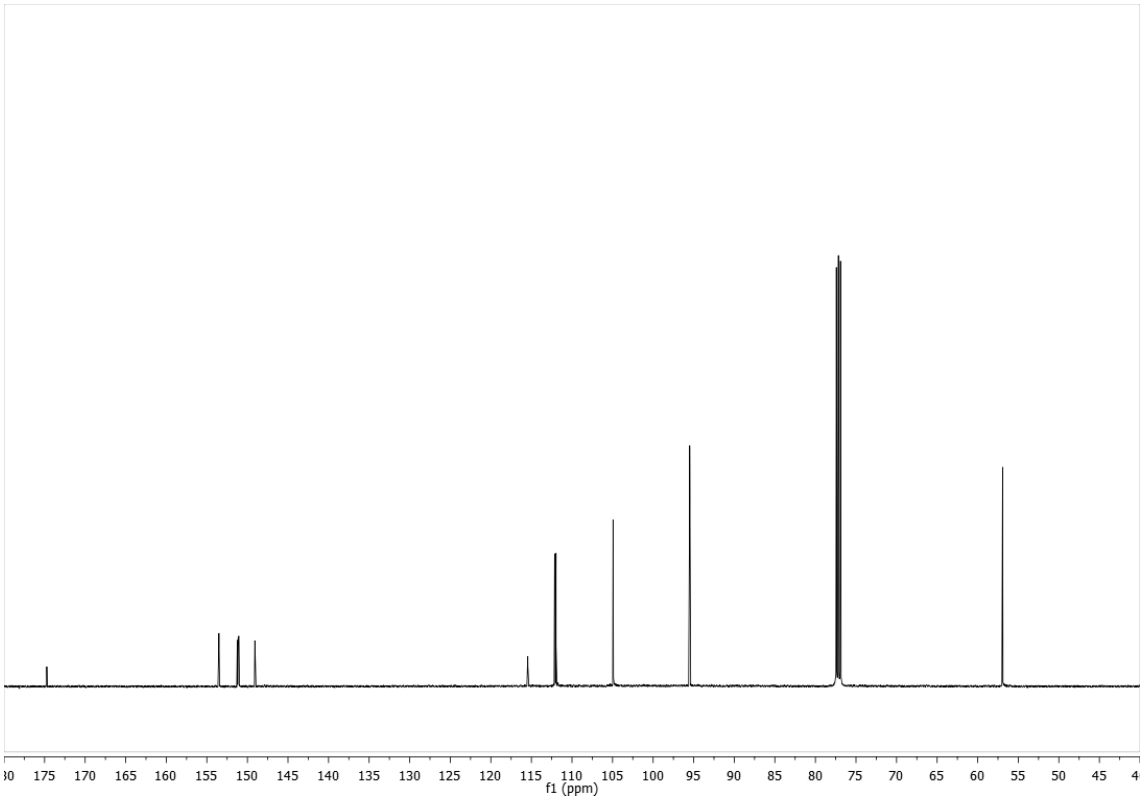

^{1}H-NMR:

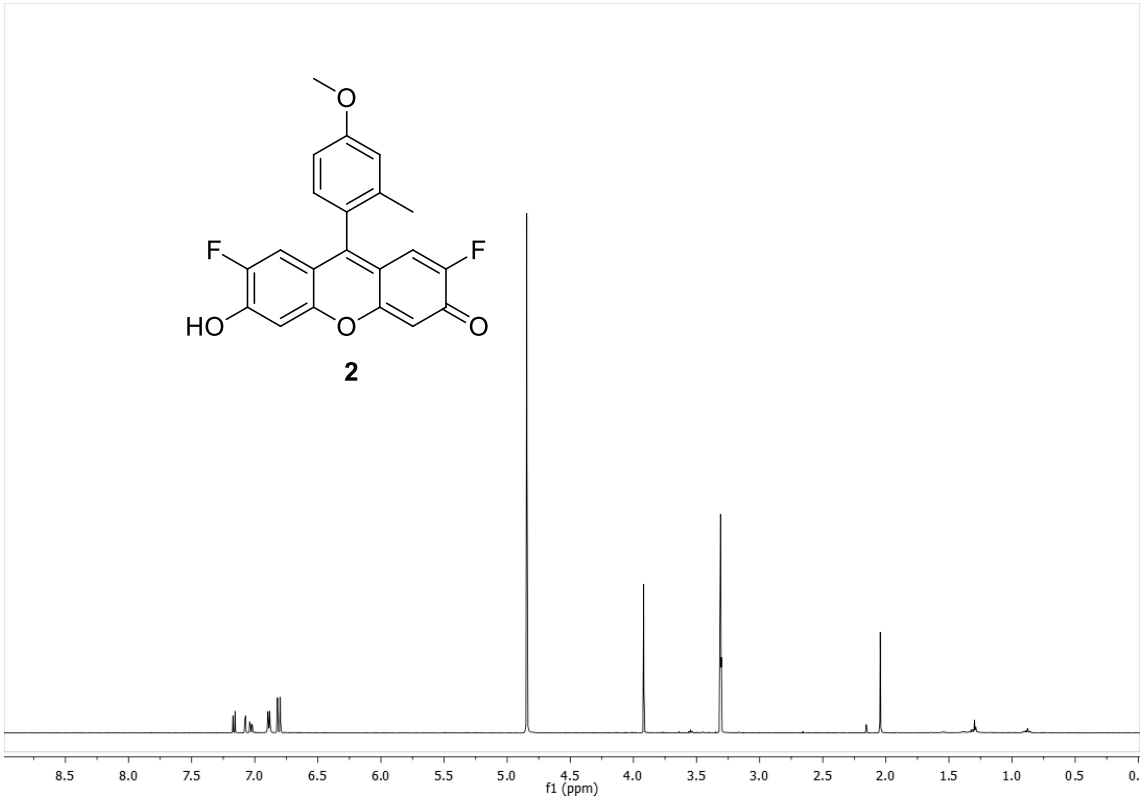

^{13}C-NMR:

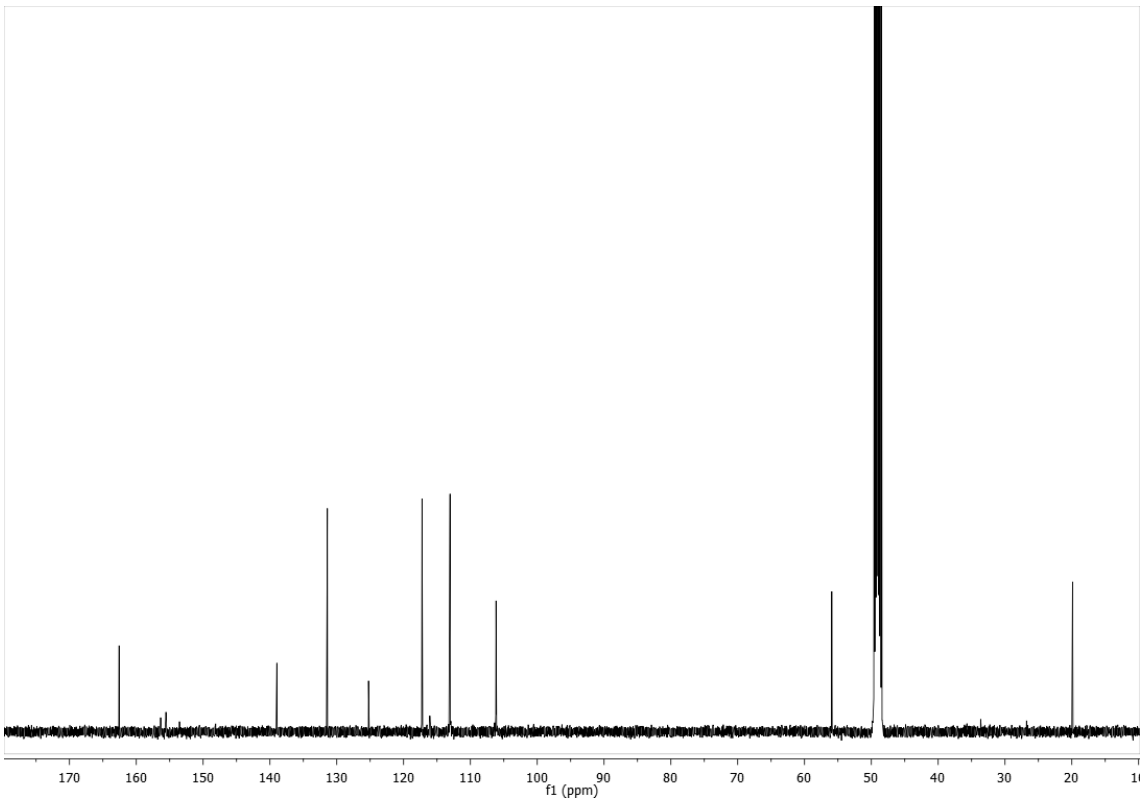

^{1}H-NMR:

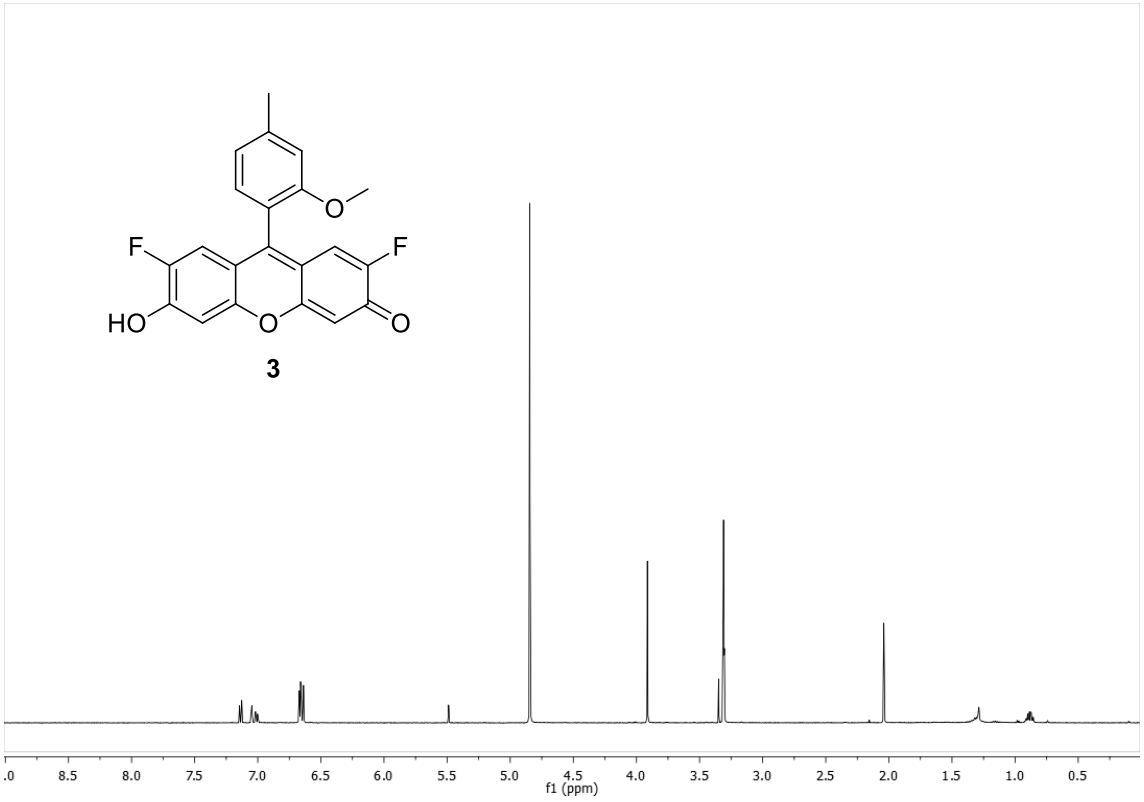

^{13}C-NMR:

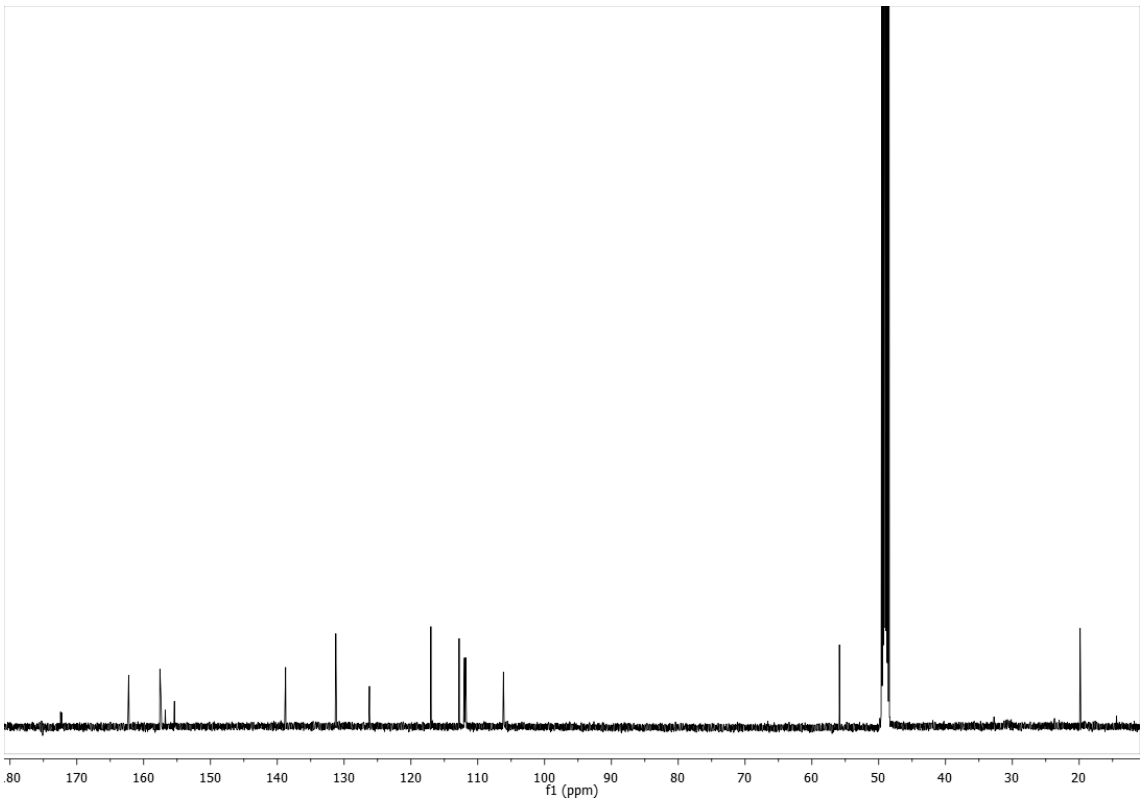

^{1}H-NMR:

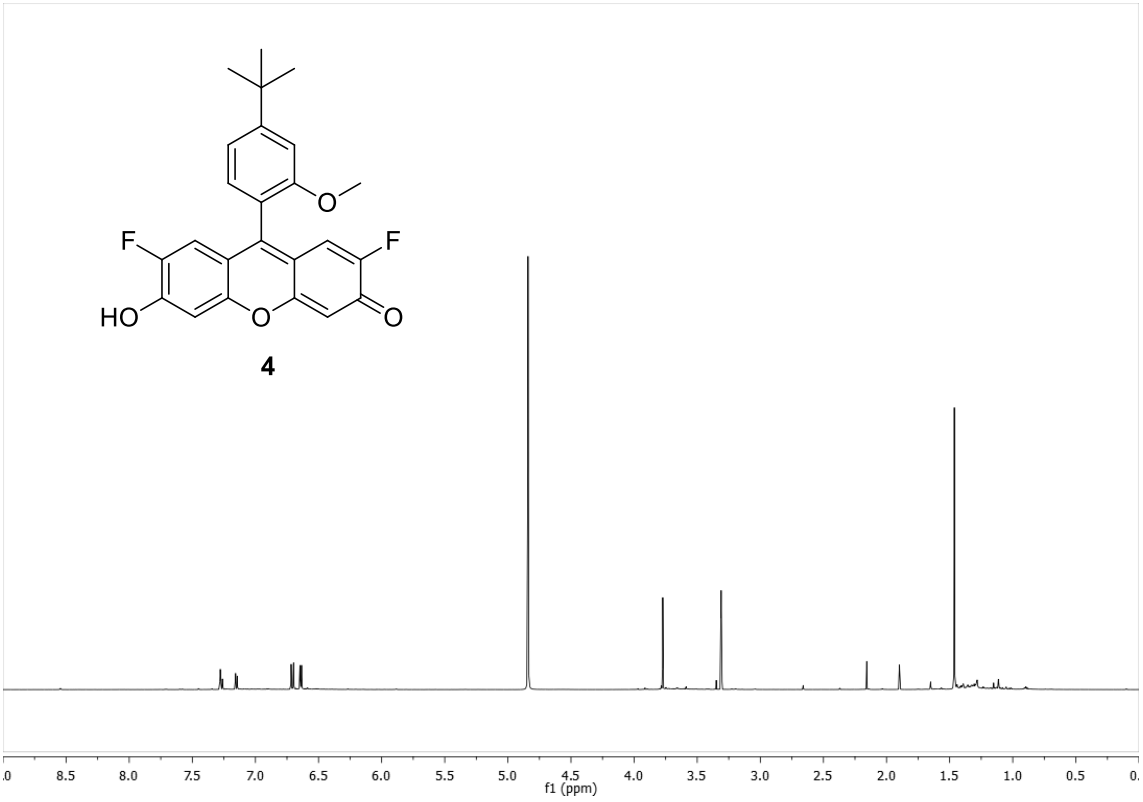

^{13}C-NMR:

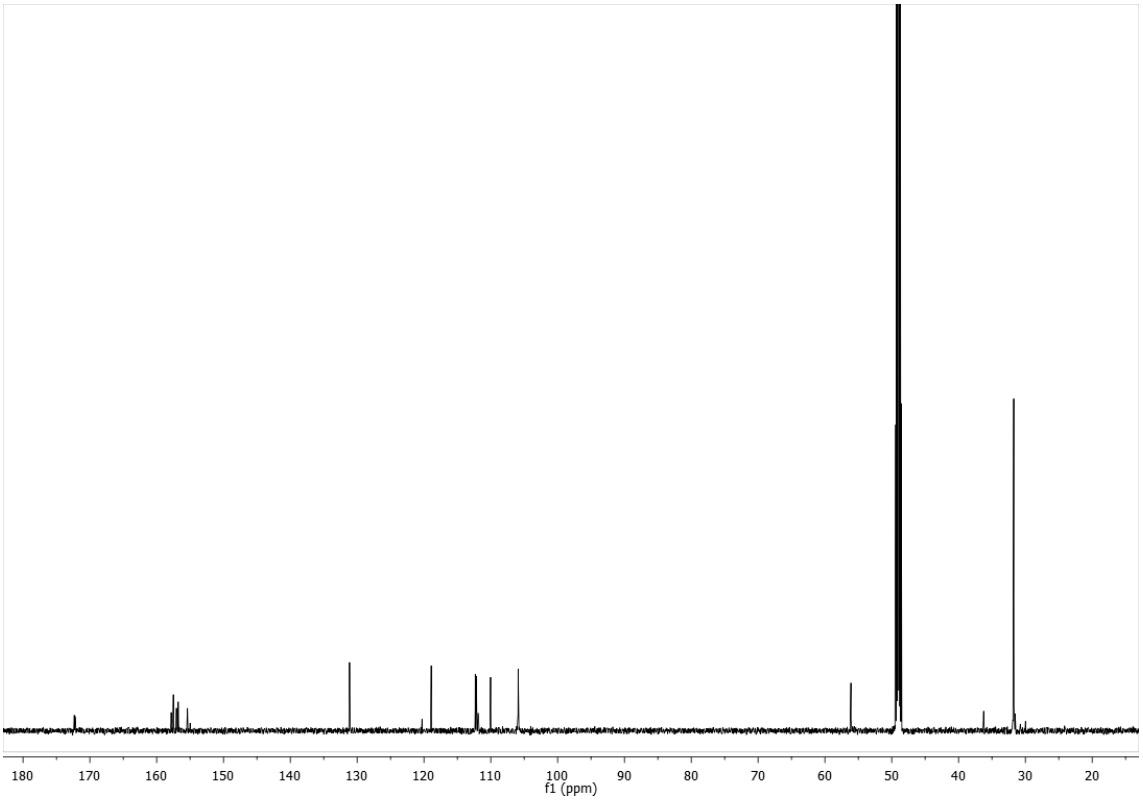

Absorption studies

If a neutral/anion system follows Beer's law, at any wavelength (λ_{abs}) and pH, the absorbance (A) is given by the expression

$$A(\mathrm{pH}, \lambda_{abs}) = C\left(\sum_i \alpha_i(\mathrm{pH}, \mathrm{p}K_{N-A}) \varepsilon_i(\lambda_{abs}) \right) d \,, \tag{S1}$$

where C is the total concentration of the dye, d is the optical path length, $\varepsilon_i(\lambda_{abs})$ is the wavelength-dependent molar absorption coefficient of the ith prototropic form of the dye, and $\alpha_i(\mathrm{p}H, \mathrm{p}K_{\mathrm{N\text{-}A}})$ is the fraction of the dye in the ith prototropic form, which depends on both pH and p$K_{\mathrm{N\text{-}A}}$.

$$\alpha_N = \frac{[H^+]}{[H^+] + K_{N-A}} \tag{S2}$$

$$\alpha_A = \frac{K_{N-A}}{[H^+] + K_{N-A}} \tag{S3}$$

Steady-State studies

The total fluorescence signal $F(\lambda_{ex}, \lambda_{em}, [H^+])$ at proton concentration $[H^+]$ due to excitation at λ_{ex} and observed at emission wavelength λ_{em} can be expressed as

$$F\left(\lambda_{ex}, \lambda_{em}, [\mathrm{H}^+]\right) = \frac{F_{min}[\mathrm{H}^+] + F_{max}K_a}{K_a + [\mathrm{H}^+]}, \tag{S4}$$

where F_{min} indicates the fluorescence signal of the neutral form of the dye and F_{max} denotes the fluorescence signal of the anion form of **2-Me-TM**. Fitting eq. S4 to the fluorescence data $F(\lambda_{ex}, \lambda_{em}, [H^+])$ as a function of $[H^+]$ yields values for K_a, F_{min}, and F_{max}.

Quantum yield values from steady-state fluorescence measurements were calculated for the anion forms using fluorescein in 0.1 M NaOH as a reference ($\phi_{fluo} = 0.95$). The quantum yield of the neutral form was obtained by fitting the steady-state fluorescence spectra to the equilibrium equation S5 once the values of ϕ_A were known.

$$F(\lambda_{ex},\lambda_{em},[H^+]) = C^{dye}K_a[\phi_N\varepsilon_N\alpha_N + \phi_A\varepsilon_A\alpha_A] \quad \text{(S5)}$$

Exited State Proton transfer reaction studies

The theory and methods of solving buffer-mediated ESPT reactions are well-established [5-8].

If the photophysical system as shown in Scheme 2 is excited by an infinitely short light pulse that does not significantly alter the concentrations of the ground-state species, then the fluorescence δ-response function, f (λ_{em},λ_{ex},t), at emission wavelength λ_{em} due to excitation at λ_{ex} is given by

$$f(\lambda_{ex},\lambda_{em},t) = p_1 e^{\gamma_1 t} + p_2 e^{\gamma_2 t} \qquad t \geq 0 \quad \text{(S6)}$$

in which eq S6 has been written in the common biexponential format,where

$$\gamma_{1,2} = \frac{-(a+c) \mp \sqrt{(c-a)^2 + 4bd}}{2} \quad \text{(S7)}$$

$a = k_{01} + k_{21} + k^B_{21}[R]$; (S8)

$b = k_{12}[H^+] + k^B_{12}[RH]$; (S9)

$c = k_{02} + k_{12}[H^+] + k^B_{12}[RH]$; and (S10)

$d = k_{21} + k^B_{21}[R]$. (S11)

[R] and [RH] are related to the total buffer concentration, C^B=[R]+[RH], by the expressions [RH] = C^B [H^+]/([H^+]+ $K_a{}^B$) and [R] = C^B $K_a{}^B$/([H^+]+ $K_a{}^B$), where $K_a{}^B$ is the dissociation constant for the reversible reaction $RH \leftrightarrow R + H^+$.

The γ factors are related to the lifetimes τ_1 and τ_2 by the expression

$$\tau_{1,2} = -\frac{1}{\gamma_{1,2}}. \quad \text{(S12)}$$

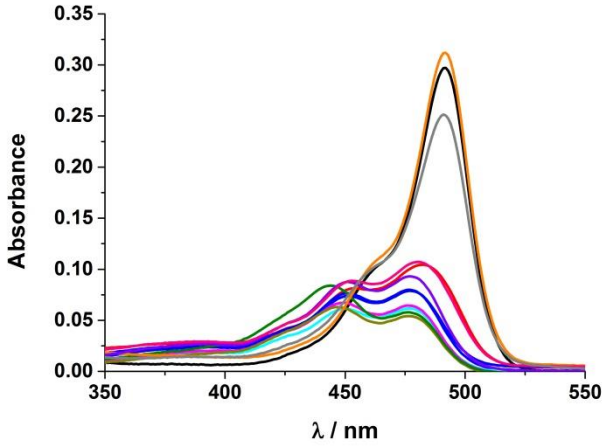

Figure S1 Absorption spectra of compound **1** (6×10^{-6} M) at different pH concentration (from 1.02 to 6.06)

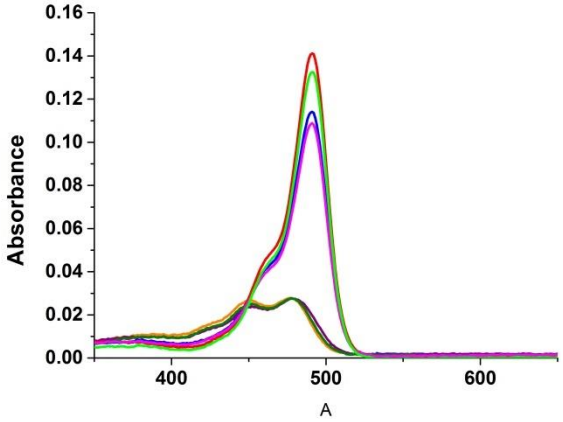

Figure S2 Absorption spectra of compound **3** (3.2 × 10-6 M) at different pH concentration (from 2.65 to 7.73)

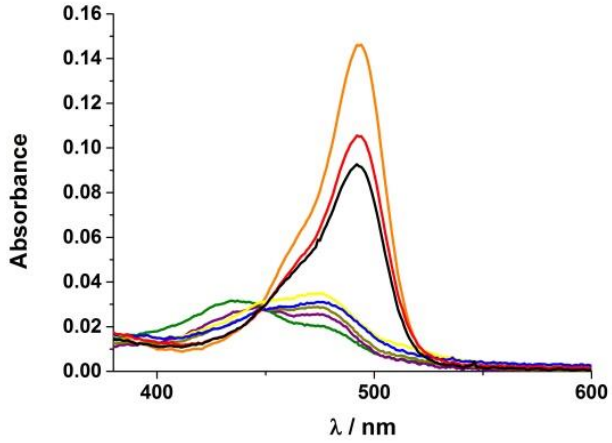

Figure S3 Absorption spectra of compound **4** (3.2×10^{-6} M) at different pH concentration (from 0.83 to 6.04)

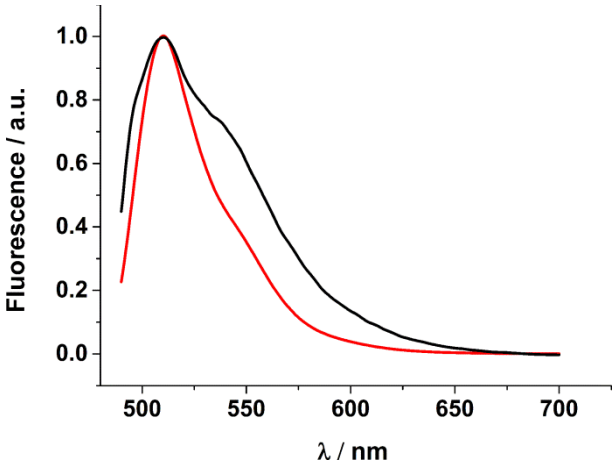

Figure S4 Normalized fluorescence emission of anion and neutral species of compound **2**

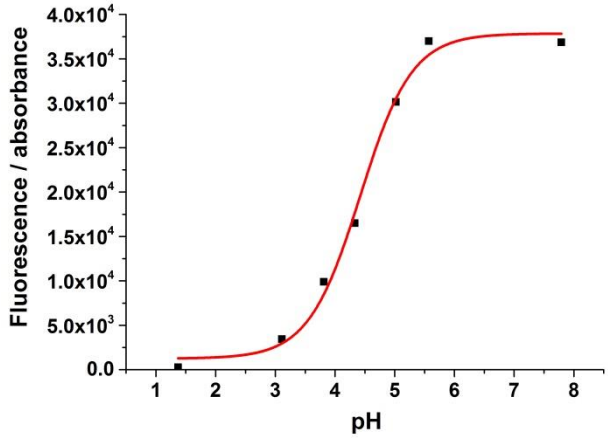

Figure S5 Curves generated by fitting (equation S) the normalized fluorescence by absorbance versus pH. Data from figure **2**

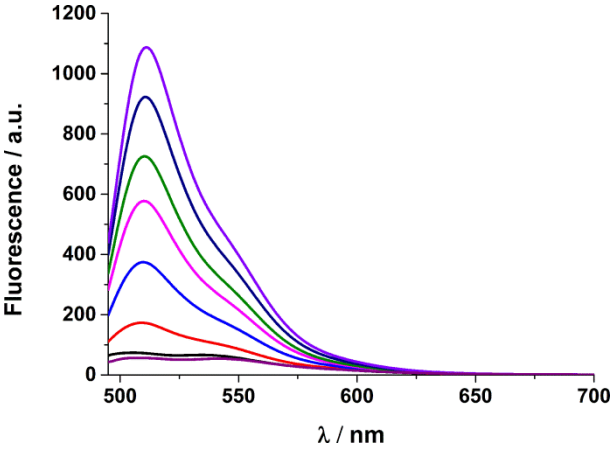

Figure S6 Fluorescence emission spectra of compound 1 (6×10^{-6} M) in acetate (255 mM) solution at different pH values (from 1.84 to 9.33)

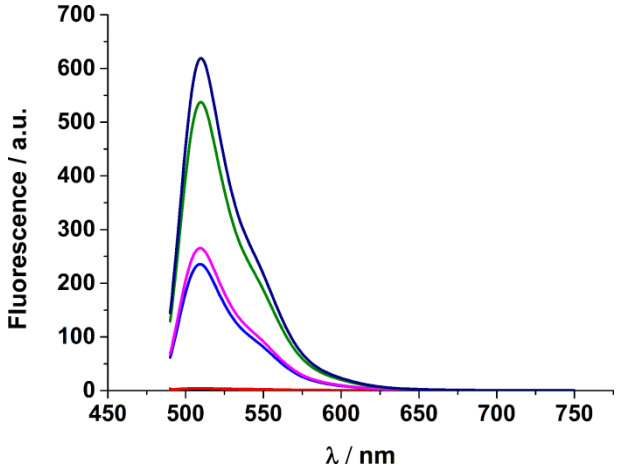

Figure S7 Fluorescence emission spectra of compound **3** (6×10^{-6} M) in acetate (255 mM) solution at different pH values (from 1.84 to 8.06)

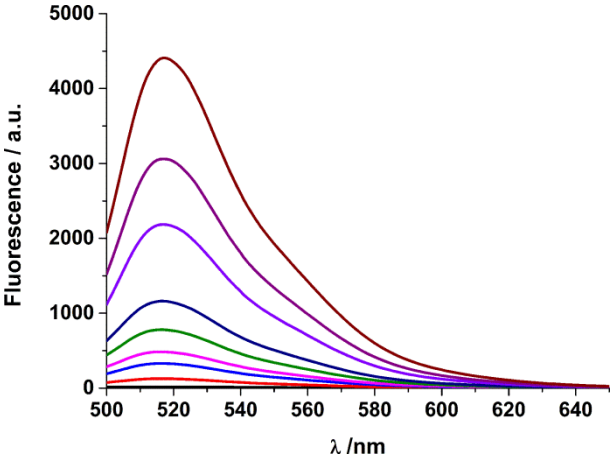

Figure S8 Fluorescence emission spectra of compound **4** (6×10^{-6} M) in acetate (340 mM) solution at different pH values (from 1.95 to 7.23)

Compound	λ_{max} abs anion	λ_{max} abs neutral	Isosbestic point	pK_a(abs)/ pK_a^*	ϕ_A/ ϕ_N	τ_{anion} /ns	$\tau_{neutral}$ /ns
1	492	445/480	457	4.66±0.06	0.79/0.12	4.80	4.00
2	492	450/478	458	4.04±0.02/4.15±0.07	0.65/0.02	3.30	0.02
3	492	450/478	450	4.78±0.02/	0.56/0.01	3.22	0.02
4	492	440/474	447	4.32±0.13 /4.27±0.03	0.64/0.04	3.75	0.008

Table S1 Photophysical parameters of all compounds.

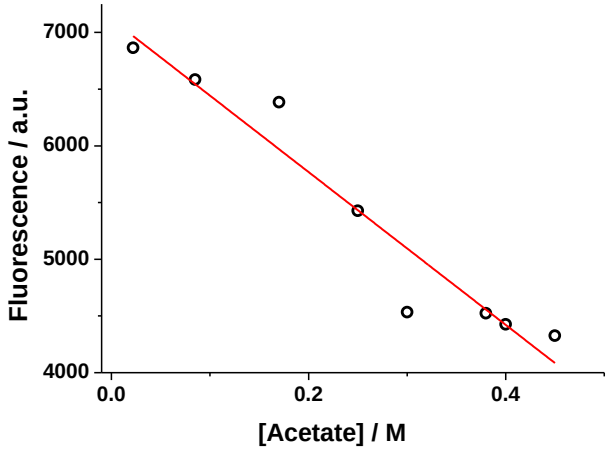

Figure S9 Dependence of the fluorescence emission to acetate concentration. In the range of acetate studied was found an acceptable linearity between fluorescence emission and acetate concentration at pH = 4.00. Linear fit obtained a $R^2 = 0.92$

Competitive studies with other anions

We checked common anions present in cell culture medium (pyruvate, glucose, phosphate and bicarbonate) at pH 4 and normal concentration in medium by time resolved fluorescence. Lifetime of the dye is not changed (table S2).

Anion	**Lifetime / ns**	**error**
bicarbonate 0.04 M	3.22	0.0018
bicarbonate 0.024 M	3.24	0.0019
pyruvate 0.00125 M	3.24	0.0025
glucose 25 mM	3.23	0.0021
phosphate 4.5 mM	3.14	0.0021
phosphate 20mM	3.15	0.0017

Table S2 Lifetime of compound **2** (6×10^{-6} M) at pH=4 in presence of different anions

Also, F^- and CN^-(table S3) were measurements. Only F^- anions show some reaction with dye, but lower than acetate (Figure S9). Normal concentration in serum for F^- [9](0.7 µM - 8 µM) is around 100 times lower than acetate concentration[10] (0.074 - 0.621 mM.) For these reasons, fluorescence or lifetime decrease in serum could be assigned exclusively to acetate.

CN^- / mM	Lifetime/ ns	error
0	3.28	0.0052
100	3.29	0.0034
200	3.29	0.0038
300	3.28	0.0030
400	3.29	0.0028
500	3.29	0.0030
600	3.29	0.0035
700	3.29	0.0029

Table S3 Lifetime of compound **2** (6×10^{-6} M) at pH=4 in presence of different CN^- concentrations

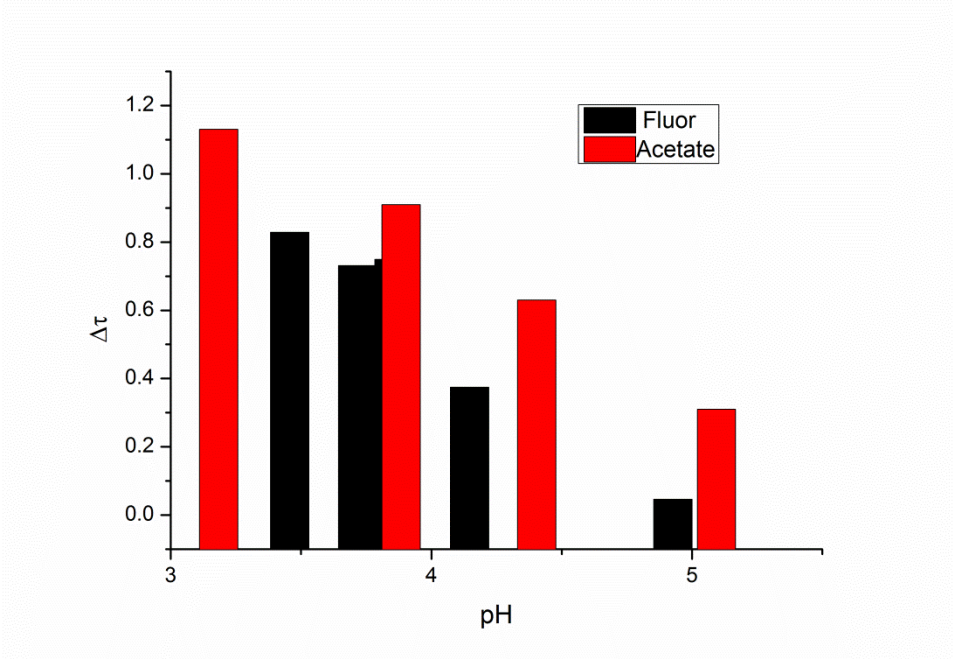

Figure S10 Lifetime changed between dye (6×10^{-6} M) without acetate or fluor anions and in presence of one of them (500 mM) at different pHs

References

[1] L. Mottram, S. Boonyarattanakalin, R.E. Kovel, B.R. Peterson, The Pennsylvania Green Fluorophore: A Hybrid of Oregon Green and Tokyo Green for the Construction of Hydrophobic and pH-Insensitive Molecular Probes, Organic Letters, 8(2006) 581-4.
[2] Z.R. Woydziak, L. Fu, B.R. Peterson, Synthesis of Fluorinated Benzophenones, Xanthones, Acridones, and Thioxanthones by Iterative Nucleophilic Aromatic Substitution, The Journal of Organic Chemistry, 77(2012) 473-81.

[3] A. Martinez-Peragon, D. Miguel, R. Jurado, J. Justicia, J.M. Alvarez-Pez, J.M. Cuerva, L. Crovetto, Synthesis and Photophysics of a New Family of Fluorescent 9-Alkyl-Substituted Xanthenones, Chemistry-a European Journal, 20(2014) 447-55.
[4] Y. Urano, M. Kamiya, K. Kanda, T. Ueno, K. Hirose, T. Nagano, Evolution of Fluorescein as a Platform for Finely Tunable Fluorescence Probes, Journal of the American Chemical Society, 127(2005) 4888-94.
[5] J.M. Alvarez-Pez, L. Ballesteros, E. Talavera, J. Yguerabide, Fluorescein Excited-State Proton Exchange Reactions: Nanosecond Emission Kinetics and Correlation with Steady-State Fluorescence Intensity, Journal of Physical Chemistry A, 105(2001) 6320-32.
[6] A. Martinez-Peragon, D. Miguel, A. Orte, A.J. Mota, M.J. Ruedas-Rama, J. Justicia, J.M. Alvarez-Pez, J.M. Cuerva, L. Crovetto, Rational design of a new fluorescent 'ON/OFF' xanthene dye for phosphate detection in live cells, Organic & biomolecular chemistry, 12(2014) 6432-9.
[7] L. Crovetto, J.M. Paredes, R. Rios, E.M. Talavera, J.M. Alvarez-Pez, Photophysics of a Xanthenic Derivative Dye Useful as an 'On/Off' Fluorescence Probe, Journal of Physical Chemistry A, 111(2007) 13311-20.
[8] L. Crovetto, A. Orte, E.M. Talavera, J.M. Alvarez-Pez, M. Cotlet, J. Thielemans, F.C. De Schryver, N. Boens, Global compartmental analysis of the excited-state reaction between fluorescein and (+/-)-N-acetyl aspartic acid, Journal of Physical Chemistry B, 108(2004) 6082-92.
[9] D.R. Taves, Normal Human Serum Fluoride Concentrations, Nature, 211(1966) 192-3.
[10] Z.T. Schug, J. Vande Voorde, E. Gottlieb, The metabolic fate of acetate in cancer, Nature Reviews Cancer, 16(2016) 708-17.